

# North Atlantic SSTs as a Link between the Wintertime NAO and the Following Spring Climate

IVANA HERCEG-BULIĆ

*Andrija Mohorovičić Geophysical Institute, Department of Geophysics, Faculty of Science, University of Zagreb, Croatia*

FRED KUCHARSKI

*Earth System Physics Section, Abdus Salam International Centre for Theoretical Physics, Trieste, Italy*

(Manuscript received 14 May 2012, in final form 26 July 2013)

## ABSTRACT

In this paper a potential seasonally lagged impact of the wintertime North Atlantic Oscillation (NAO) on the subsequent spring climate over the European region is explored. Supported by the observational indication of the wintertime NAO–spring climate connection, a modeling approach is used that employs the International Centre for Theoretical Physics (ICTP) atmospheric general circulation model (AGCM) as a stand-alone model and that is also coupled with a mixed layer ocean in the North Atlantic. Both observational and modeled data indicate a pattern of sea surface temperatures (SSTs) in North Atlantic as a possible link between wintertime NAO and climate anomalies in the following spring. The SST pattern is associated with wintertime NAO and persists through the following spring. It is argued that these SST anomalies can affect the springtime atmospheric circulation and surface conditions over Europe. The atmospheric response is recognized in observed as well as in modeled data (mean sea level pressure, temperature, and precipitation). Additionally, an impact on springtime storm activity is found as well.

It is demonstrated that the SST anomalies associated with wintertime NAO persist into the subsequent spring. These SST anomalies enable atmosphere–ocean interaction over the North Atlantic and consequently affect the climate variability over Europe. Although it has a relatively weak impact, the described mechanism provides a temporal teleconnection between the wintertime NAO and subsequent spring climate anomalies.

## 1. Introduction

The North Atlantic Oscillation (NAO) is the most energetic mode of climate variability over the wintertime Atlantic–European sector in the Northern Hemisphere. Since it was defined by Sir Gilbert Walker (Walker 1924; Walker and Bliss 1932) as a simultaneous increase and decrease of sea level atmospheric pressure at the Azores and Iceland, respectively, it has been investigated extensively. The origin of low-frequency variability and potential predictability of the NAO is still under discussion, with some results supporting the hypothesis that the NAO variability may be attributed to internal atmospheric dynamical processes (e.g., Jung et al. 2011), like, for example, the stratosphere–troposphere coupling (Scaife et al. 2005)

and Rossby wave–breaking events (Woollings et al. 2008), while other results indicate that forcing mechanisms may also play a role, [e.g., El Niño–Southern Oscillation (ENSO); e.g., Greatbatch and Jung (2007)].

The NAO is the major factor governing air–sea interactions over the Atlantic, and NAO-related surface atmospheric conditions strongly affect the ocean through sensible and latent heat exchanges resulting in ocean temperature anomalies projecting onto the North Atlantic SST tripole pattern (Cayan 1992a; Deser and Timlin 1997; Seager et al. 2000). Since the NAO is most powerful during the winter (from December till March), the associated SST pattern is strongest in late winter. Frankignoul (1985) reported a typical *e*-folding time of the pattern of about 3–5 months at the ocean surface. The persisting signal in the ocean affects the atmosphere by SST anomalies that modify air–sea heat fluxes, enabling a coupling between the ocean and the atmosphere (Frankignoul 1985; Frankignoul et al. 1998; Kushnir et al. 2002). For example, Mosedale et al. (2006) have demonstrated that the

---

*Corresponding author address:* Ivana Herceg-Bulić, Andrija Mohorovičić Geophysical Institute, Dept. of Geophysics, Faculty of Science, University of Zagreb, Horvatovac 95, Zagreb, Croatia.  
E-mail: ihercegb@gfz.hr

SST tripole in the Atlantic Ocean can provide a small yet statistically significant feedback on the NAO. Air–sea interactions in the North Atlantic region have also been analyzed by other studies as well as by numerical modeling experiments (e.g., Bladé 1997; Cayan 1992a,b; Deser and Blackmon 1993; Kushnir 1994; Barsugli and Battisti 1998; Peng and Whitaker 1999; Bretherton and Battisti 2000; Czaja and Marshall 2000; Watanabe and Kimoto 2000; Rodwell and Folland 2002; Kucharski and Molteni 2003; Cassou et al. 2007; Eden and Jung 2001; Eden and Willebrand 2001; Greatbatch and Jung 2007; Visbeck et al. 2003; Herceg-Bulić and Kucharski 2011).

Two-way interaction between the North Atlantic and the atmosphere was proposed by Bjerknes (1964), who hypothesized that on an interannual time scale the North Atlantic SST anomalies are mainly forced by the atmosphere, while on longer time scales the NAO could be influenced by the Atlantic Ocean. More recent studies have also indicated the possibility that SST variations in the North Atlantic may influence NAO variability (e.g., Rodwell et al. 1999; Kushnir et al. 2002; Kushnir and Held 1996; Seager et al. 2000; Watanabe and Kimoto 2000; Czaja and Frankignoul 1999; Wang et al. 2004; Frankignoul et al. 2011; Scaife et al. 2011), implying a possible predictable oceanic influence on the NAO.

Kushnir et al. (2002) provide a review of processes through which midlatitude SST variations can influence the atmosphere. They find that two processes are primarily responsible for generating a midlatitude atmospheric response to SST anomalies: a baroclinic atmospheric response that can generate barotropic atmospheric variations through associated changes in the storm tracks, and a linear thermodynamic interaction in which SST adjustment reduces the thermal damping of the atmospheric variability (Barsugli and Battisti 1998). Ferreira and Frankignoul (2005) examine the first of these mechanisms in a simplified atmospheric model coupled to a slab-ocean model. They show that the SST response to NAO variability can generate an atmospheric response that feeds back positively to the original NAO variability through associated shifts in transient eddy activity. In nature, both of these processes may work together.

The influence of the NAO on the climate of the Northern Hemisphere is well documented in the available literature, particularly for the winter season when this phenomenon dominates the climate variability on hemispheric as well as on regional scales (see, e.g., Hurrell et al. 2003 for an overview). Fluctuations in the meridional pressure gradient (caused by variations in pressure over the subpolar and subtropical regions of the North Atlantic) modulate westerly winds blowing

across the Atlantic Ocean. Accordingly, the advection of mild and humid air to Europe is modified. Such changes in the atmospheric circulation significantly determine European climate with strong impacts on storm tracks, temperature, and precipitation. For example, atmospheric processes linked to NAO account for half of the interannual variability in the surface temperature during winter over northern Europe (Rodwell et al. 1999), as well as a third of the interannual variability in precipitation (Hurrell 1996). In general, winters with a positive NAO index are associated with anomalously dry conditions over central and southern Europe and wet conditions over northern Europe, although the greatest variations in the precipitation may occur over the Atlantic, as pointed out by Scaife et al. (2005). The NAO signal is also detectable in surface temperatures with a positive NAO associated with warmer conditions in northern and central Europe and a cooler than usual Mediterranean region. The NAO is strongest in the winter, but it is also evident during the whole year in the Northern Hemisphere (Barnston and Livezey 1987), although it is less dominant and has a smaller amplitude and spatial extent. Accordingly, the associated fluctuations of surface pressure, temperature, and precipitation occur throughout the year [e.g., Folland et al. (2009) discuss the summer NAO].

Although the literature concerning the winter NAO is abundant, there is a lack of studies exploring the impact of the wintertime NAO on the climate of subsequent seasons. Namely, the wintertime NAO can interact with slower components of the climate system (e.g., ocean, land surface, soil, sea ice, and snow), inducing persistent surface anomalies that may affect the atmosphere via surface feedback mechanisms resulting in an atmospheric response that is lagged for several months from the initial forcing. For example, Rigor et al. (2002) hypothesized a seasonal memory of the preceding winter Arctic Oscillation (AO) based on summertime sea ice concentration that is strongly correlated with the AO index of the previous winter. Furthermore, by correlation and linear regression analysis based on the National Centers for Environmental Prediction–National Center for Atmospheric Research (NCEP–NCAR) reanalysis dataset, Ogi et al. (2003) showed that wintertime NAO generates persistent anomalies in snow cover, sea ice, and ocean SSTs in the circumpolar regions, and suggested that these anomalies may affect the summertime atmospheric circulation. In such a way, the NAO may have an impact on hot and dry summers in Europe, maintaining favorable conditions for the initialization and longer duration of extreme heat conditions (e.g., Fischer et al. 2007; Ogi et al. 2003; Vautard et al. 2007). From that point of view, better understanding of

mechanisms that enable seasonally lagged NAO effects and their possible impacts on seasonal forecasts are of great interest.

The aim of this study is to provide some new aspects and evidence of a seasonally lagged signal in the climate variability of the North Atlantic–European region that is associated with the wintertime NAO. For this purpose, observational data were analyzed. Also, numerical experiments employing a stand-alone AGCM as well as the model coupled with a mixed layer ocean were performed to explain the physical mechanism. The paper is organized as follows. We begin in section 2 with a short description of the data, model, and methods used in this study. In section 3, an analysis of observed data indicating a lagged connection between the wintertime NAO and the following spring climate over the North Atlantic–European region is presented. Furthermore, in this section the results based on numerical integrations underpinning the hypothesis of a wintertime NAO–spring climate connection are also provided. Section 4 offers a discussion of the presented results and a concluding assessment of the relevance of the delayed NAO’s impact on climate over the North Atlantic–European region.

## 2. Data, model, and methodology

### a. Observational data

The observational datasets used in this study include monthly mean precipitation, mean sea level pressure (SLP), surface air temperature (SAT), and SST. The precipitation and air temperature data are provided by the Climatic Research Unit (CRU) as gridded monthly datasets (CRU-TS3.1 and CRUTEM3, respectively) for the 1901–2009 time period that covers the global land surface at  $0.5^\circ \times 0.5^\circ$  resolution (New et al. 2000; Mitchell et al. 2004; Brohan et al. 2006). Sea level pressure analysis was performed using HadSLP2 dataset, a reconstruction of SLP carried out by the Hadley Centre (Allan and Ansell 2006). The Hadley Centre Sea Level Pressure Dataset (HadSLP1) covers both land and sea globally at  $5^\circ \times 5^\circ$  resolution. It is an update of the Hadley Centre’s earlier Global Mean Sea Level Pressure dataset (Barnett and Parker 1997). For SST data we used the National Oceanic and Atmospheric Administration’s (NOAA) Extended Reconstructed Sea Surface Temperatures, version 3 (ERSST.v3), dataset,<sup>1</sup> a reconstruction of global sea surface temperature (Smith et al. 2008).

The analysis of observational data covers a 100-yr-long time period (1901–2000).

### b. ICTP AGCM

The modeled data are obtained by 150-yr-long numerical integrations using International Centre for Theoretical Physics (ICTP) AGCM, version 41, with a horizontal resolution of T30 and eight vertical levels (T30-L8; documentation and verification available online: <http://users.ictp.it/~kucharsk/speedy-net.html>). It is a model of intermediate complexity with parameterizations including short- and longwave radiation, large-scale condensation, convection, surface fluxes of momentum, heat and moisture, and vertical diffusion. The model also has a facility to be coupled with a thermodynamic slab-ocean layer that mimics air–sea interaction (see, e.g., Kucharski et al. 2006; Herceg-Bulić and Kucharski 2011). A more detailed description of the model can be found in Kucharski et al. (2006) and Kucharski et al. (2013). Molteni (2003) shows that the model is capable of simulating atmospheric flow realistically as well as the forced and internal components of atmospheric interdecadal variability, with a mean state that is closer to the observed climatology during the boreal winter than during the summer. On seasonal-mean time scales that are strongly influenced by the NAO, the greatest variability coincides with the observations, but with underestimated amplitude. According to Kucharski and Molteni (2003), the ICTP AGCM reproduces the structure of the internal atmospheric NAO in good agreement with the observations. Also, the ICTP AGCM simulates reasonably well the atmospheric response to the SST trends in tropical oceans (Bracco et al. 2004).

For the purposes of this study, we use results of the following model experiments:

- (i) NATL—150-yr-long run of the model coupled with a thermodynamic slab-ocean layer over the North Atlantic (north of  $20^\circ\text{N}$ ) generating SST anomalies through changes in the atmospheric fluxes of heat; outside the slab ocean, SSTs were set to climatological (only seasonally varying) values with linear smoothing between these regions; the mixed-layer depth is a function of latitude only and varies from 40 m in the tropical regions to 60 m in the extratropical regions;
- (ii) CLIM—150-yr-long run of a stand-alone AGCM; SSTs were set globally to the climatological values; and
- (iii) CLIM+MAM—100-yr-long idealized run with the stand-alone ICTP AGCM forced with time-invariant March–May (MAM) SST anomaly in the North Atlantic [MAM SST is the December–February

<sup>1</sup> Provided by the NOAA/OAR/ESRL PSD, Boulder, Colorado (<http://www.esrl.noaa.gov/psd/>).

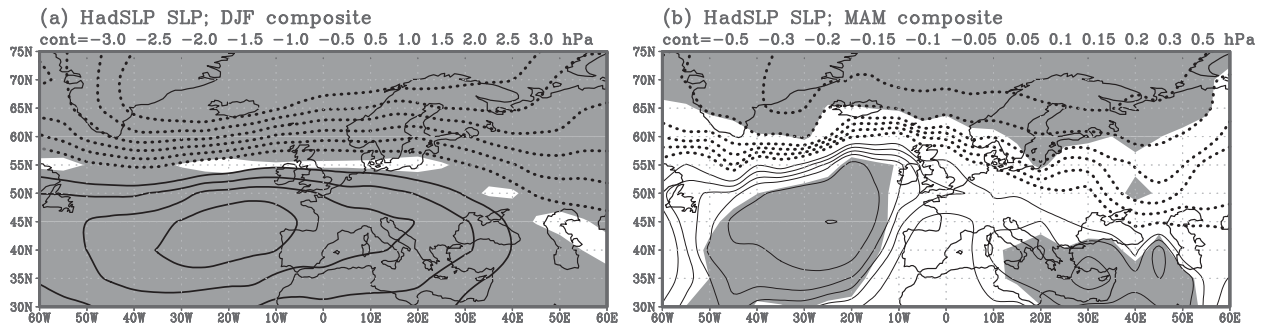


FIG. 1. NAO composite of observed SLP (HadSLP, hPa) anomalies for (a) DJF and (b) MAM. Contours are set at 0.5, 1.0, 1.5, 2.0, 2.5, and 3.0 hPa in (a) and 0.05, 0.1, 0.15, 0.2, 0.3, and 0.5 hPa in (b). Negative values are dashed. Shaded areas exceed the 90% confidence level using a two-tailed  $t$  test. DJF and MAM composites are based on the same winter (DJF) NAO index categorization.

(DJF) NAO-related composite that is simulated by the mixed layer in the NATL experiment). Outside the North Atlantic, SSTs were set to climatological values.

In all runs, sea ice is expressed as fractions and set to the climatological values (only seasonally varying).

### c. Methodology

Here, we analyze precipitation, SLP, SAT, and SST anomalies calculated by subtracting the mean annual cycle. The long-term mean of every calendar month was subtracted from each individual month. Seasonal anomalies [January–March (JFM), February–April (FMA), MAM, etc.] were calculated as 3-month averages. The seasons of the most interest for this study are winter (DJF) and spring (MAM).

To show the spatial pattern of the NAO impact, composite and correlation analyses were employed. The domain under study is the North Atlantic–European region. Composite analysis was performed considering the polarity and strength of the winter (DJF) NAO index. The NAO index used here is the principal component (PC) based NAO index obtained as time series of the leading empirical orthogonal function (EOF) of DJF SLP anomalies calculated over the 20°–80°N, 90°W–40°E area, as defined by Hurrell et al. (2003). Assuming that the first EOF represents a canonical positive NAO event, positive (negative) NAO years were defined as those years with standardized PC1 greater (smaller) than 0.5 (−0.5). The threshold of 0.5 has been chosen as a compromise between identifying an NAO event and retaining as much data as possible for the analysis. Composites of observed data are constructed upon a PC-based NAO index provided by NCAR’s Climate Analysis Section (<http://climatedataguide.ucar.edu/guidance/hurrell-north-atlantic-oscillation-nao-index-pc-based>). To produce composites of data obtained by ICTP AGCM integrations, the categorization into positive

and negative NAO years was made considering a PC-based NAO index that was calculated by using simulated SLP. Following that, composites of seasonal anomalies associated with positive and negative NAOs were calculated. Since the composites have revealed a roughly linear response to opposite NAO phases (i.e., the same spatial pattern but with the anomalies having reversed signs) and in order to increase the statistical significance of the analysis, we are considering the mean response (computed as the positive NAO composite minus the negative NAO composite divided by 2). The correlation analysis is performed in this study to present spatial correlation maps for certain fields. The correlations were calculated between time series of the NAO index and time series of the considered parameter at every grid point. The statistical significance of composites and correlation maps was evaluated by a two-tailed  $t$  test. To assess the impact of winter NAO on spring (MAM) climate, we have examined composites and correlation patterns based on NAO categorization taking into account the DJF NAO index.

## 3. Results

In this section we show results concerning the wintertime NAO impact on climate variability in the North Atlantic–European region during the following spring. The observational analyses are presented in section 3a, while results based on numerical integrations are discussed in section 3b.

### a. Observational indication of wintertime NAO–spring climate connection

The composite of observed mean sea level pressure anomalies related to the winter NAO (Fig. 1a) reveals a well-known NAO pressure dipole with increased SLP over the southern part and decreased SLP over the northern part of the domain, resulting in a strong meridional

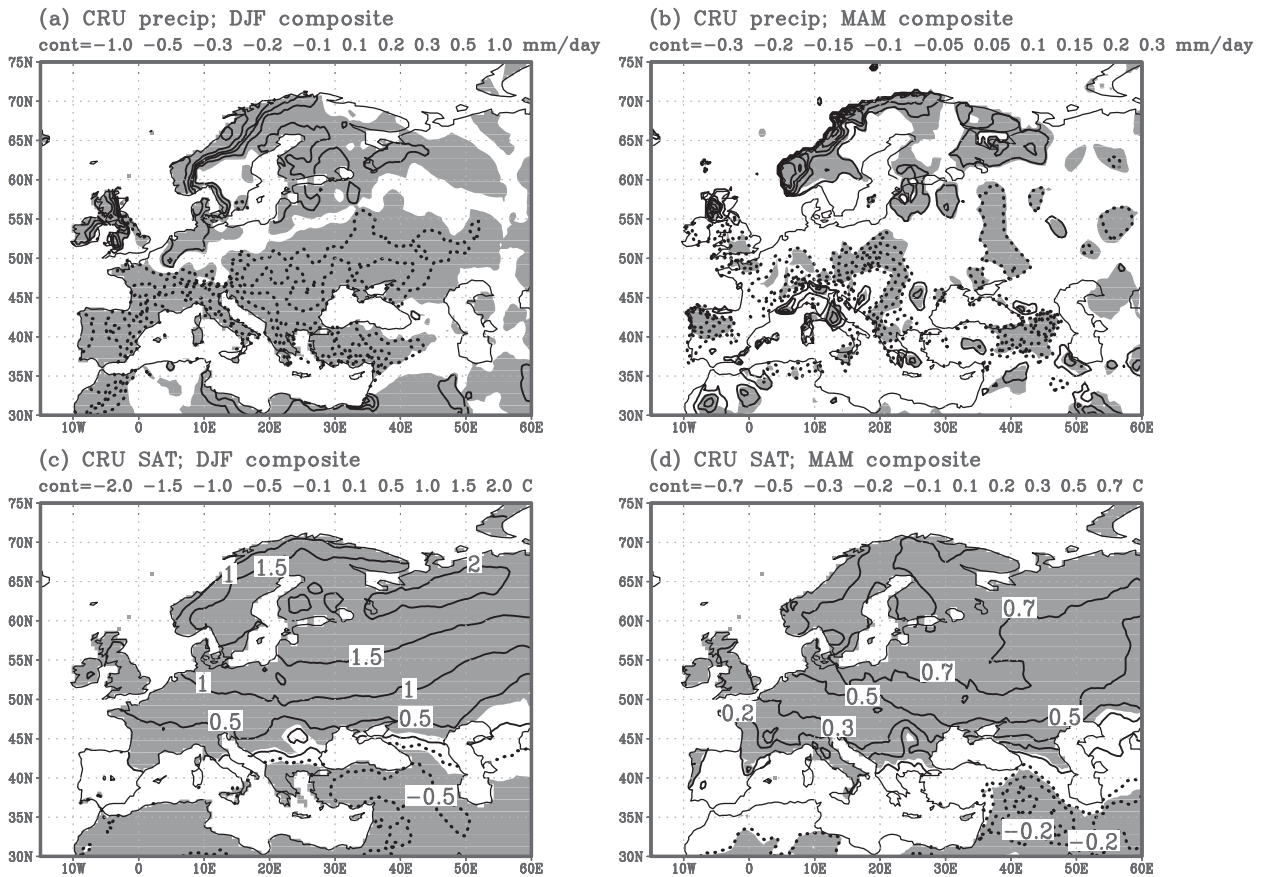


FIG. 2. NAO composites of CRU precipitation anomalies ( $\text{mm day}^{-1}$ ) for (a) DJF and (b) MAM and CRU temperature anomalies ( $^{\circ}\text{C}$ ) for (c) DJF and (d) MAM. Contours are at 0.1, 0.2, 0.3, 0.5, and  $1.0 \text{ mm day}^{-1}$  in (a); 0.05, 0.1, 0.15, 0.2, and  $0.3 \text{ mm day}^{-1}$  in (b);  $0.1^{\circ}$ ,  $0.5^{\circ}$ ,  $1.0^{\circ}$ ,  $1.5^{\circ}$ , and  $2^{\circ}\text{C}$  in (c); and  $0.1^{\circ}$ ,  $0.2^{\circ}$ ,  $0.3^{\circ}$ ,  $0.5^{\circ}$ , and  $0.7^{\circ}\text{C}$  in (d). Negative values are dashed. Shaded areas exceed the 90% confidence level using a two-tailed  $t$  test. DJF and MAM composites are based on the same winter (DJF) NAO index categorization.

SLP gradient around  $55^{\circ}\text{N}$ . The pattern similar to that for the winter season persists into the following spring (Fig. 1b). During boreal spring, both the spatial extent and the amplitude of SLP anomalies are smaller compared to those for the winter (please note the different contour intervals in Figs. 1a,b). Although with substantially smaller statistical significance than for DJF, the main features of the DJF pattern are still kept in the MAM pattern as well as in the meridional SLP gradient (with a spatial correlation between the DJF and MAM patterns of 0.91).

Observed precipitation and temperature responses to the winter NAO are presented in Fig. 2. The winter (DJF) composite reveals a bipolar precipitation pattern (Fig. 2a) that is consistent with the pressure pattern in Fig. 1a. During the positive (negative) NAO, the northern part of the considered area is associated with more abundant (reduced) DJF precipitation anomalies, while precipitation over the southern part is reduced (increased). The largest precipitation response is found

along western coasts (Iberian Peninsula, Scandinavia, Great Britain) with absolute values of anomalies sporadically exceeding  $1 \text{ mm day}^{-1}$ . The spatial pattern of the MAM precipitation response is changed to some extent, but still reveals a bipolar distribution (Fig. 2b) resembling the DJF response. Generally, the response is considerably weaker with the MAM amplitude, which is approximately half of the DJF amplitude ( $0.5 \text{ mm day}^{-1}$ ). Nevertheless, there is a distinct spatial similarity between the DJF and MAM precipitation composites.

Temperature also shows a robust response to the NAO. Here, as a consequence of enhanced (suppressed) westerly flow across the North Atlantic that increases (decreases) the advection of relatively warm air over much of Europe, positive (negative) SAT anomalies are found for positive (negative) NAOs over most of the considered domain (Fig. 2c). The response is strongest over northern Europe (with maximal absolute values exceeding  $2^{\circ}\text{C}$ ). Consistently with the SLP pattern in

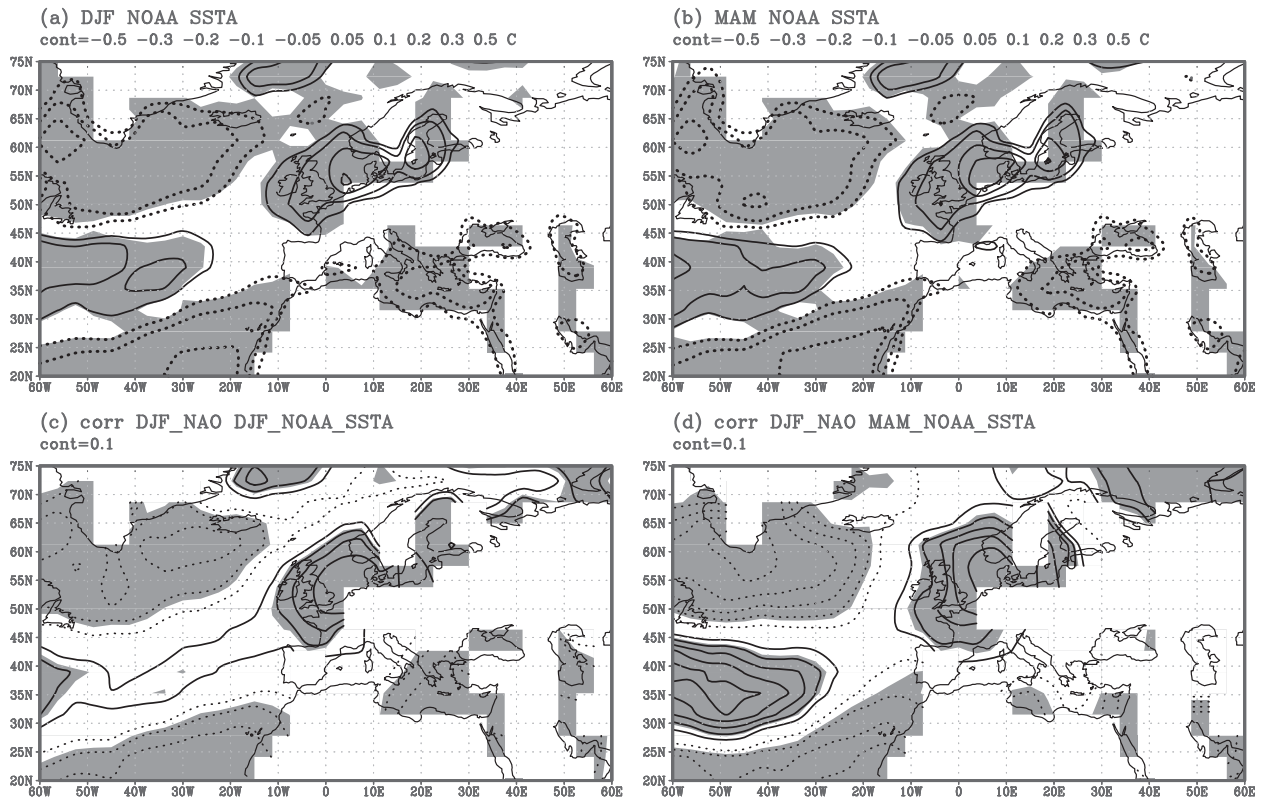


FIG. 3. SST anomaly composites for (a) DJF and (b) MAM and correlation maps between the DJF NAO index and (c) DJF and (d) MAM NOAA SSTs. Contours are at 0.05, 0.1, 0.2, 0.3, and 0.5 in (a) and (b); the contour interval is 0.1 in (c) and (d). Negative values are dashed. Shaded areas exceed the 90% confidence level using a two-tailed  $t$  test.

Fig. 1, the MAM SAT response (Fig. 2d) is weaker (the amplitude is almost 3 times less than that for DJF), but with similar spatial pattern to that obtained for the DJF season.

The winter composite pattern of SSTs associated with a positive DJF NAO shows the well-known tripole SST pattern over the North Atlantic consisting of cold SST anomalies south of Greenland and in the subtropics accompanied by warm anomalies following the extension of the Gulf Stream (Fig. 3a). Also, warm anomalies are found near the western European coast with the center over the North Sea, while the Mediterranean Sea is colder than usual. Such an SST anomaly distribution corresponds to the leading SST variability pattern during boreal winter with a tripolar spatial structure driven by changes in the surface wind and air–sea heat exchanges associated with the NAO, all of which is consistent with the results of many other studies (e.g., Cayan 1992a,b; Visbeck et al. 2003).

A similar SST pattern is also kept during the MAM season (Fig. 3b), suggesting its seasonal persistence. To demonstrate the potential connection between the SST pattern and DJF NAO events, maps showing correlations

between time series of the DJF NAO index and SST anomalies in North Atlantic are presented (Figs. 3c,d). An instantaneous correlation pattern (DJF NAO–DJF SST; Fig. 3c) has correlations that are consistent with the above-mentioned tripole pattern, indicating the connection between the DJF NAO events and the underlying ocean. A similar pattern of statistically significant (and even increased) correlation coefficients still exists during the MAM season (Fig. 3d), indicating a lagged connection (DJF NAO–MAM SST).

We have applied the same procedure to SSTs of different periods (arbitrarily chosen) and obtained patterns consistent with those in Fig. 3 (not shown). Although with different values of correlation coefficients (due to different periods of calculation), those results also imply significant correlation between the DJF NAO and North Atlantic SSTs with stronger lagged (DJF NAO–MAM SST) correlations than instantaneous (DJF NAO–DJF SST) correlations. The presented results demonstrate that the ocean integrates atmospheric forcing associated with the NAO during boreal winter, resulting in the maximum response during the subsequent spring. The following analysis will investigate the possibility that

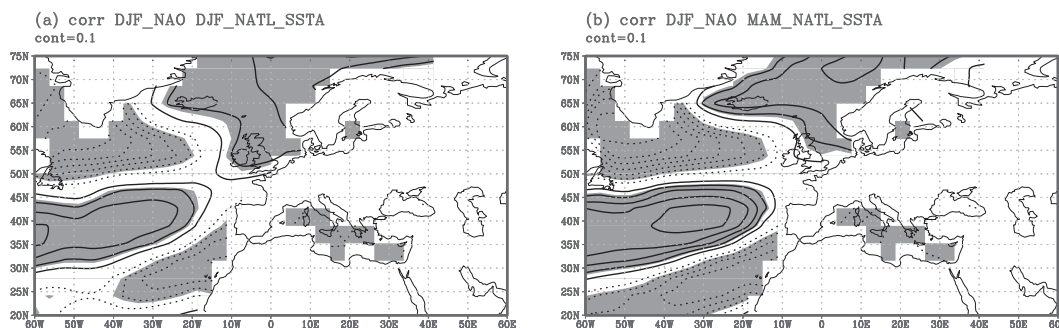


FIG. 4. Correlation map between the DJF NAO index and simulated (NATL) SSTs for (a) DJF and (b) MAM. The contour interval is 0.1. Negative values are dashed. Shaded areas exceed the 90% confidence level using a two-tailed  $t$  test.

those oceanic SST anomalies can generate the MAM atmospheric response seen in Figs. 1 and 2.

#### *b. Model interpretation of wintertime NAO–spring climate connection*

In the previous section, the observational indication of a potential connection between the spring climate variability and the preceding wintertime NAO is demonstrated. Since the SST pattern associated with the wintertime NAO persists into boreal spring, it is possible that springtime atmospheric anomalies are (at least partially) a result of the atmospheric response to that SST forcing. To examine that interaction, we have performed numerical experiments using the ICTP AGCM model. The simulation (denoted as NATL) is performed with the ICTP AGCM coupled with a mixed layer ocean in the North Atlantic. Since the slab ocean does not have any ocean dynamics, the SSTs in North Atlantic’s slab layer are generated by atmospheric forcing solely and do not reflect the impacts of some other processes occurring in nature (like ocean currents and seasonally varying ocean depth). The results obtained in the NATL experiment are compared with the results of the same model with no mixed ocean layer (i.e., stand-alone AGCM simulations) forced with climatological SSTs (CLIM run), as well as with observations.

The maps showing correlations calculated between the DJF NAO index and the modeled SST anomalies (Fig. 4) have patterns similar to those for observations in Fig. 3, but with greater values of correlation coefficients and broader spatial extent of the statistically significant values. The DJF correlation map in Fig. 4a indicates a tripolar SST pattern in the North Atlantic resembling the observed one (Fig. 3a), although it is slightly shifted northward. The MAM correlation map is also reproduced reasonably well (cf. Figs. 3d and 4b), particularly considering the relatively coarse horizontal resolution of the model and the simplicity of the mixed ocean layer.

Additionally, the NATL experiment yields significant correlations between DJF NAO and MAM SST (Fig. 4b) with almost the same spatial pattern as that for the DJF season (Fig. 4a). The observed (Fig. 3) and modeled (Fig. 4) correlation maps reveal spring SST patterns with spatial similarities to those found for the DJF season. Accordingly, the atmosphere may be influenced by this spring SST pattern. However, the atmospheric response to Atlantic forcing is quite complex, as discussed by Kushnir et al. (2002 and references therein). According to the findings of Sutton et al. (2001), the low-latitude atmospheric response is associated with low-latitude SST anomalies, while the high-latitude response is associated with both extratropical and tropical SST anomalies with a nonlinear interaction between them. Since the slab ocean in our study extends into the subtropical North Atlantic (20°N), there is a possibility that the subtropical Atlantic also has an effect. Therefore, we have repeated the NATL experiment with the northern boundary of the slab-ocean layer at 30°N. Obtained results (not presented) revealed that there is no significant impact of that 10° latitudinal shift. This does not rule out the possibility that the tropical Atlantic also may affect the midlatitude atmosphere, but by this additional run we have ascertained that the signal obtained in NATL is associated with the extratropical Atlantic with no significant influence from the tropics.

Here, we are focusing on an extratropical SST pattern consisting of two bands of SST anomalies: one that is negatively correlated with the DJF NAO (placed south of Greenland, around 60°N) and the other with the SST anomalies that are positively correlated with the DJF NAO (placed around 35°N). To test the relationship between the wintertime NAO and our proposed dipole SST pattern, the seasonal correlation ( $r$ ) between the DJF NAO index and the SST index (SSTI) of every particular month (starting with the preceding January and going forward) is calculated (Fig. 5) for both

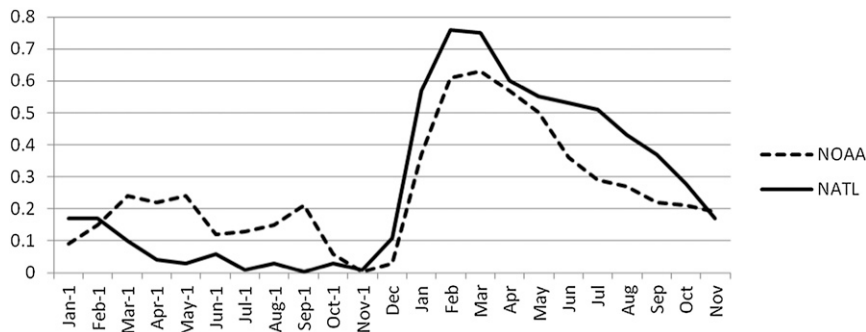


FIG. 5. Monthly correlations between the SST index (SSTI; see text for definition) and the DJF NAO index based on observed SSTs (NOAA; dashed line) and modeled SSTs (NATL; solid line). Values greater than 0.2 for NOAA and 0.16 for NATL exceed the 95% confidence level for zero correlation.

observed SSTs (NOAA, dashed line) and modeled SSTs (NATL, solid line). The SSTI is a measure of the strength of the dipole (depicted in Figs. 3 and 4) and is calculated as a difference between the area-averaged SSTs in ( $30^{\circ}$ – $45^{\circ}$ N,  $20^{\circ}$ – $60^{\circ}$ W) and ( $50^{\circ}$ – $65^{\circ}$ N,  $20^{\circ}$ – $60^{\circ}$ W). For observed SSTs (dashed line in Fig. 5), the correlation with the DJF NAO index is almost zero for December. Hereafter, it increases considerably, reaching its peak in February and March (with  $r$  values of 0.61 and 0.63, respectively). After that, the correlation weakens during April and May (but still with  $r$  values greater than 0.5) and drops in June (0.36), with continuous decrease afterward. The lagged correlations presented here are consistent with the study of Frankignoul and Hasselmann (1977) based on a stochastic model. Their results show that large-scale SST anomalies may be attributed to short time-scale atmospheric forcing and have an  $e$ -folding time of the order of half a year.

The correlations for modeled data (solid line in Fig. 5) mainly achieve higher values than those for the observations, but they indicate the same temporal dependence (the correlation between the NOAA and NATL cycles in Fig. 5 is 0.89). All correlations quoted above are at least 95% statistically significant. Figure 5 depicts a clear asymmetry in the lead–lag correlation between the DJF NAO and SSTI for both the observations and NATL simulation, with larger correlations if the DJF NAO is leading the SSTI and is strongly suggestive of a DJF NAO forcing of the following early spring SSTI.

After May, the modeled correlations do not decrease as rapidly as observed, indicating longer SST seasonal persistence in the model than in the observations. This is probably due to the simple slab ocean used in the study, which has no seasonal cycle for the mixed layer depth while it can be quite shallow in the North Atlantic during the summer (de Boyer-Montégut et al. 2004). Additionally, the slab model has no ocean dynamics, so modeled

SST anomalies cannot be dispersed as effectively as in the real ocean (or in a model with ocean dynamics) where SST anomalies may be advected by the mean current in the mixed layer reducing the local  $e$ -folding time scale (Frankignoul 1985).

Figure 5 also implies a few points of importance for this study. First, there is a significant correlation between the observed DJF NAO index and SSTI for January and February, suggesting a connection between the wintertime NAO and the underlying sea after a wintertime NAO has occurred. Second, the SST pattern is seasonally persistent (since there are also significant correlations between the DJF NAO and the SSTIs of the following seasons). Moreover, the simple mixed ocean layer (which is just a crude representation of the real ocean) satisfactorily reproduces the observed SSTs in the North Atlantic and their seasonal persistence, as well as the annual cycle of the connection between the DJF NAO index and the SST dipole. Figure 5 also supports the selection of MAM as a representative season for this study: the SST dipole persists into the spring (and consequently may influence the atmosphere during that season), MAM is the season with the greatest  $r$  values with no month overlapping with any of the months constituting the DJF season, and the differences between the observed and modeled  $r$  values in Fig. 5 are minimal for March, April, and May (i.e., for these months, the model is in the best accordance with the observations regarding the DJF NAO–SSTI correlation). The above-presented results show that the model reproduces the SST dipole consistently with the observations for both the DJF and MAM seasons.

Next, we examine the structure of the modeled atmospheric variations in MAM that are associated with the previous DJF NAO. The wintertime and springtime atmospheric responses to DJF NAO in the NATL experiment are presented in Fig. 6. Taking into account the

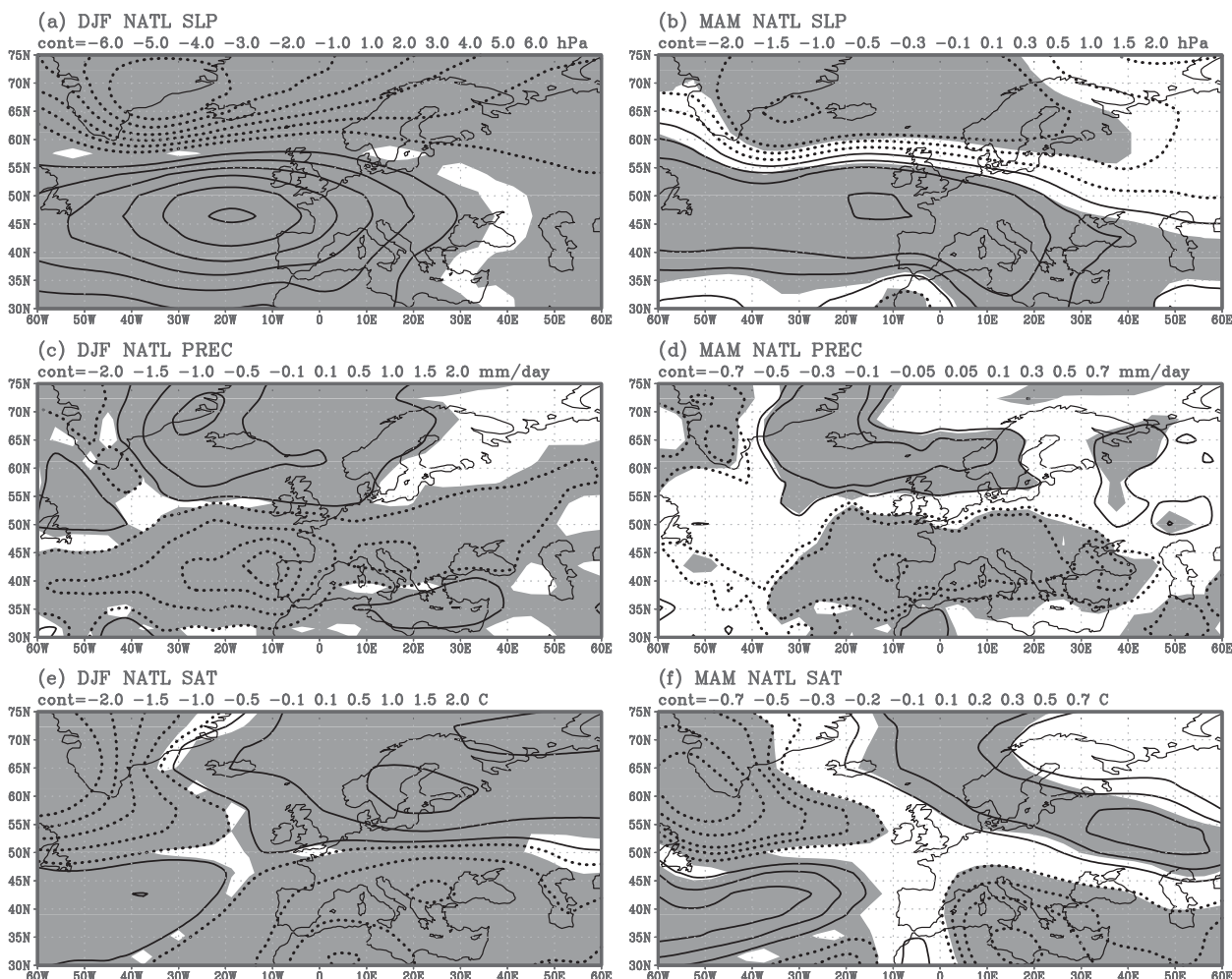


FIG. 6. NAO composites of simulated (NATL) SLP anomalies (hPa) for (a) DJF and (b) MAM, precipitation anomalies ( $\text{mm day}^{-1}$ ) for (c) DJF and for (d) MAM, and temperature anomalies ( $^{\circ}\text{C}$ ) for (e) DJF and (f) MAM. Contours are at 1.0, 2.0, 3.0, 4.0, 5.0, and 6.0 hPa in (a); 0.1, 0.3, 0.5, 1.0, 1.5, and 2.0 hPa in (b); 0.1, 0.5, 1.0, 1.5, and 2.0  $\text{mm day}^{-1}$  in (c); 0.05, 0.1, 0.3, 0.5, and 0.7  $\text{mm day}^{-1}$  in (d);  $0.1^{\circ}$ ,  $0.5^{\circ}$ ,  $1.0^{\circ}$ ,  $1.5^{\circ}$ , and  $2.0^{\circ}\text{C}$  in (e); and  $0.1^{\circ}$ ,  $0.2^{\circ}$ ,  $0.3^{\circ}$ ,  $0.5^{\circ}$ , and  $0.7^{\circ}\text{C}$  in (f). Negative values are dashed. Shaded areas exceed the 95% confidence level using two-tailed  $t$  test. The DJF and MAM composites are based on the same winter (DJF) NAO index categorization.

relatively coarse resolution of the model, it reproduces the structure of the DJF NAO reasonably well (cf. Figs. 1a and 6a), although the modeled amplitude is twice that of the observations. Modeled SLP composites show a typical NAO bipolar structure over the North Atlantic and Europe during the winter with a strong meridional gradient around  $57^{\circ}\text{N}$  (Fig. 6a). The pressure pattern during the spring (Fig. 6b) is weaker but bears a strong resemblance to that of DJF (with a spatial correlation of 0.91). Although the model overestimates the observed SLP response and the NAO pattern is shifted slightly northward in the model, both the DJF and MAM dipole structures are reproduced with resemblance to the observations (Fig. 1).

The simulated precipitation (Figs. 6c,d) and temperature responses (Figs. 6e,f) reproduce the same main

features as are found in the observations (cf. Figs. 2 and 6). Over Europe, a positive DJF NAO phase is associated with more abundant (sparse) winter precipitation accompanied by increases (decreases) in temperature north (south) of  $55^{\circ}\text{N}$  during both the winter and the subsequent spring (Figs. 6c–f). The strongest precipitation responses over land are simulated across the same areas as are found for the observed precipitation (southern Europe and the western coast of Scandinavia). However, the model produces the most intense precipitation response over the North Atlantic Ocean. Based on numerical simulations with the coupled Hadley Centre Atmospheric Model, version 3 (HadAM3), Scaife et al. (2005) also indicate North Atlantic as the area with the strongest NAO-related precipitation signal. The MAM precipitation and temperature composites (Figs. 6d,f)

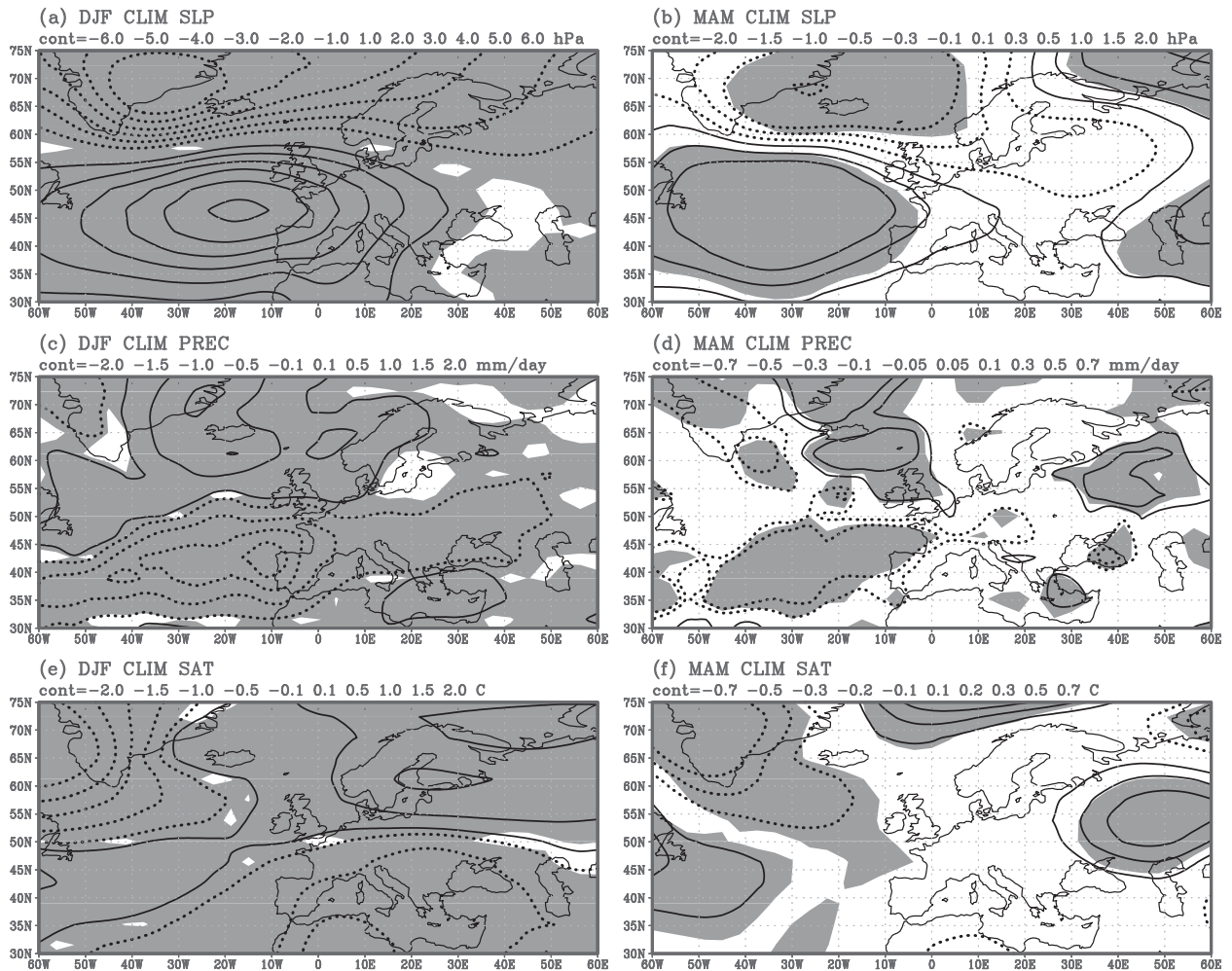


FIG. 7. As in Fig. 6, but for the climatological run (CLIM).

have bipolar structures that resemble their counterparts during the DJF season (Figs. 6c,e), but with decreased amplitudes (in the same way as found for the observations).

The observed and modeled atmospheric patterns (Figs. 1, 2, and 6) reveal a spatial similarity between the DJF and MAM atmospheric responses. In addition, composites and correlation maps of SSTs (Figs. 3–5) indicate that the SST pattern associated with the wintertime NAO persists until the subsequent spring and this SST pattern may have an instantaneous impact on the atmosphere. To explore this potential interaction, we analyze the results from the CLIM experiment (ICTP AGCM forced with climatological SSTs). Since there is no ocean layer in this experiment, the atmospheric circulation simulated in the CLIM run is not affected by air–sea interactions and is, rather, a result of atmospheric processes solely. Accordingly, the comparison of atmospheric anomalies simulated in the NATL and

CLIM runs may signify a potential impact of the SST forcing. Figure 7 reveals that CLIM's contemporaneous atmospheric signal (NAO composites for the DJF season in Figs. 7a,c,e) reflects almost in detail the NATL signal (Figs. 6a,c,e), with strong spatial correlation between them (e.g., the correlation between DJF SLP and MAM SLP is 0.99). Since DJF composites are based on the selection of DJF NAO indices associated with the first EOF of modeled SLP, both composites actually represent the DJF NAO pattern as simulated by the model (Figs. 6a and 7a). Indeed, accompanying precipitation and SAT fields are consistent with the SLP fields (Figs. 6c,e and 7c,e). While the DJF SLP pattern is reproduced similarly in both the NATL and CLIM experiments over the whole domain, the respective MAM patterns show some differences. Over the ocean, the structure of the MAM CLIM simulation (Fig. 7b) is still very similar to that of MAM NATL over the same region (Fig. 6b), indicating a persistent NAO due to purely

TABLE 1. Spatial correlations calculated between HadSLP, CLIM SLP, and NATL SLP over the region 30°–75°N, 0°–60°E.

Model/data	Corr
CLIM DJF, NATL DJF	0.99
HadSLP DJF, CLIM DJF	0.93
HadSLP DJF, NATL DJF	0.92
HadSLP DJF, HadSLP MAM	0.91
NATL DJF, NATL MAM	0.88
HadSLP MAM, NATL MAM	0.81
CLIM DJF, NATL MAM	0.33
CLIM DJF, CLIM MAM	0.11
HadSLP MAM, CLIM MAM	0.05

atmospheric processes. However, substantial differences between these two experiments are found in their responses over Europe. The MAM CLIM signal over Europe (Fig. 7b) is considerably weaker with smaller areas of statistical significance compared to the MAM NATL signal (Fig. 6b). The same is also true for precipitation and temperature fields (Figs. 6d,f and 7d,f).

With the goal of comparing the observed (HadSLP in Fig. 1) and modeled SLP fields (NATL SLP in Figs. 6a,b and CLIM SLP in Figs. 7a,b) for the DJF and MAM seasons, spatial correlations are calculated over the European domain (30°–75°N, 0°–60°E; Table 1). According to Table 1, patterns closest to the observed SLP are obtained for the DJF season (for both the CLIM and NATL runs), as a consequence of the NAO definition based upon a particular structure of SLP anomalies. The MAM SLP patterns of both the HadSLP and NATL datasets project onto the corresponding DJF SLP pattern, resulting in a high correlation between the DJF and MAM SLP composites (0.91 and 0.88, respectively). On the contrary, this is not the case for the CLIM run, which reveals a considerable difference between DJF SLP and

MAM SLP over Europe, resulting in a weak and statistically insignificant spatial correlation between them (0.11). Over Europe, the NATL experiment reproduces an MAM SLP pattern that is much closer to the observed one than is found for the CLIM experiment (the HadSLP MAM–NATL MAM correlation is 0.81, while the HadSLP MAM–CLIM MAM correlation is only 0.05).

It is shown here that the wintertime NAO is simulated in the same way in both the NATL and CLIM experiments. However, there are substantial differences between the MAM NATL and MAM CLIM composites over Europe. To explore the significance of that difference, the CLIM MAM SLP composite (Fig. 7b) is subtracted from the NATL MAM SLP composite (Fig. 6b) and is presented in Fig. 8. A statistically significant distinction over southern Europe and part of northern Europe is obtained. This result points out that the considerable discrepancy between the outputs of the NATL experiment and the CLIM experiment occurs over Europe. Both of these experiments are performed with the same AGCM and the only difference between them is that the model is coupled with the slab ocean in the NATL run, suggesting the influence of the ocean mixed layer.

Figures 6 and 7 indicated that springtime atmospheric patterns over Europe may be affected by North Atlantic SSTs. To verify this indication, we performed an additional experiment (denoted as CLIM+MAM). It is an idealized run with the AGCM forced with a constant MAM SST composite in the North Atlantic and climatological SSTs elsewhere. The MAM SST pattern is taken from the NATL experiment (i.e., it is simulated during the MAM season by the ocean mixed layer in the NATL run). In such a way, the CLIM+MAM run

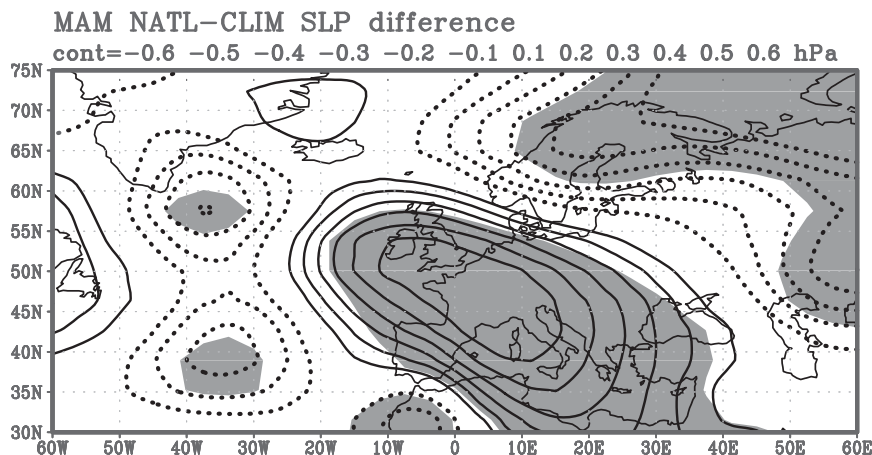


FIG. 8. Difference between MAM SLP composites (hPa) obtained in the NATL and CLIM experiments. Contours are at 0.1, 0.2, 0.3, 0.4, 0.5, and 0.6 hPa. Negative values are dashed. Shaded areas exceed the 90% confidence level using a two-tailed  $t$  test.

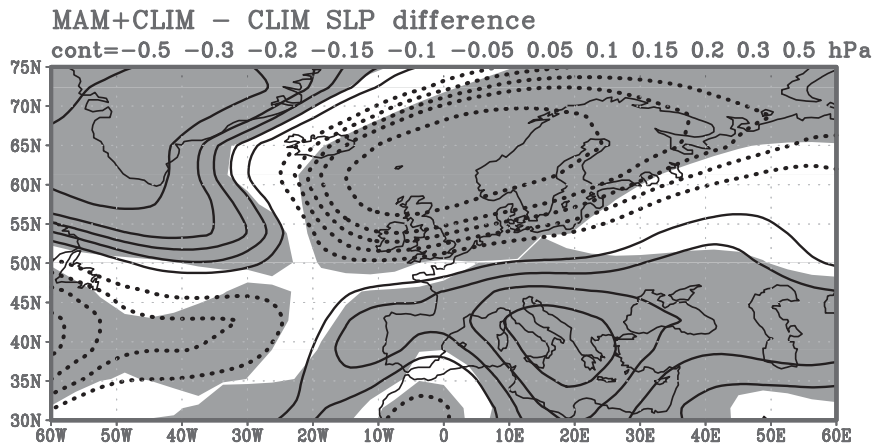


FIG. 9. Difference between averaged MAM SLP from the MAM+CLIM run (the run with the stand-alone ICTP AGCM forced with a constant MAM SST anomaly composite in the North Atlantic; composite is taken from the NATL run considering DJF NAO categorization) and MAM SLP from the CLIM run (the experiment with climatological SSTs everywhere). Contours are at 0.05, 0.1, 0.15, 0.2, 0.3, and 0.5 hPa. Negative values are dashed. Shaded areas exceed the 90% confidence level using a two-tailed  $t$  test.

reflects the model's sensitivity to the prescribed extratropical SST pattern. The difference between the MAM\_SST and CLIM runs (Fig. 9) depicts the bipolar structure of the SLP anomalies over Europe with negative (positive) values over the north (south). Over Europe, this pattern is similar to the one shown in Fig. 8 (the spatial correlation in the region  $30^{\circ}$ – $75^{\circ}$ N,  $0^{\circ}$ – $60^{\circ}$ E is 0.63). However, some differences between Figs. 9 and 8 are also evident, particularly in the western parts (where the difference map in Fig. 8 is less significant). This may indicate that coupled air–sea interactions are important and cannot exactly be reproduced by imposing a constant SST anomaly (e.g., Bretherton and Battisti 2000), although sampling may also contribute, to some extent, to the differences. Nevertheless, the CLIM+MAM experiment shows that the atmosphere is sensitive to extratropical SST anomalies in spring, and that the response in the European region is broadly consistent with the interpretation that the winter NAO related mixed layer SST anomalies in the North Atlantic existing during the MAM season can influence simulated European climate anomalies.

According to some previous studies, the main cyclone tracks are also affected by NAO phases. Thus, during a positive NAO phase, the strengthening of the activity is found in the area from Newfoundland into northern Europe and weakening is found to the south (e.g., Rogers 1990, 1997). The findings of Serreze et al. (1997) and Deser et al. (2000) indicate more intense and frequent storms in the vicinity of Iceland and the Norwegian Sea are associated with a positive NAO. To sketch out one of the possible consequences of the time-lagged NAO's

impact, its effect on storm activity is estimated here by the variance (for periods of 1–30 days) of the geopotential height at 850 hPa (varGH850; Fig. 10). The amplitudes of the DJF climatological mean of varGH850 show zonally elongated maxima extending across the North Atlantic from the eastern coast of Greenland to the Norwegian Sea (Fig. 10a). This area is characterized with high temporal variability in geopotential heights and, therefore, preferred trajectories for weather systems. A similar pattern is retained during the MAM season, but with smaller amplitudes (Fig. 10b). The winter composite of the varGH850 anomalies around the DJF NAO categorization (Fig. 10c) indicates that a positive NAO is associated with increased storm activity from Greenland, across Iceland, to the Norwegian Sea, and decreased storm activity to the south (centered approximately over the Azores). For the MAM composite (Fig. 10b), the changes in storm activity are not as pronounced as for the winter season, but still somewhat increased (decreased) activity in the northern (southern) part of North Atlantic is depicted. This result indicates that the wintertime NAO has an impact on spring storm activity over the North Atlantic in a manner similar to that during the preceding winter. Although this effect is much weaker than during the winter, it is still statistically significant over some parts of the ocean.

#### 4. Discussion and conclusions

In this paper we explore the potential role of extratropical SST anomalies in the temporal teleconnection between the wintertime NAO and subsequent spring

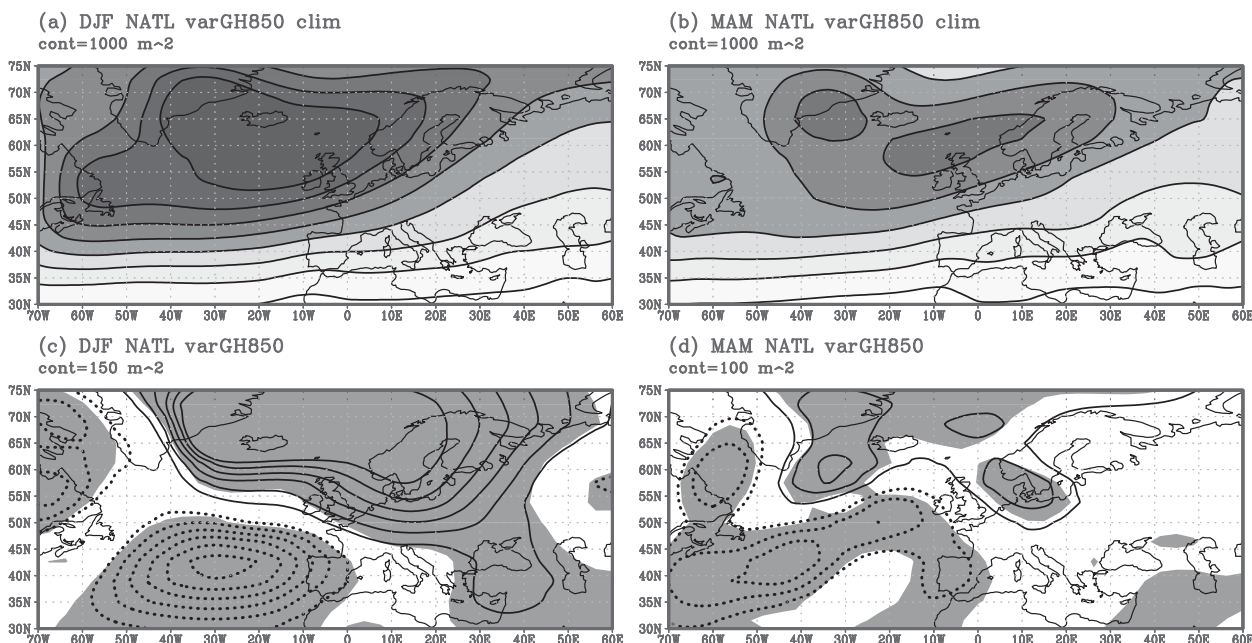


FIG. 10. Climatology of simulated (NATL) variance of daily geopotential height at 850 hPa ( $\text{varGH}$ ;  $\text{m}^{-2}$ ) for (a) DJF and (b) MAM, and NAO composites of  $\text{varGH850}$  ( $\text{m}^{-2}$ ) for (a) DJF and for (b) MAM. The contour intervals are at  $1000 \text{ m}^{-2}$  in (a) and (b),  $150 \text{ m}^{-2}$  in (c), and  $100 \text{ m}^{-2}$  in (d). Negative values are dashed. Shaded areas exceed the 90% confidence level using a two-tailed  $t$  test. DJF and MAM composites are based on the same winter (DJF) NAO index categorization.

climate variability over the North Atlantic–European region. Observational evidence for a wintertime NAO–spring climate connection is presented using composite and correlation maps constructed upon PC-based DJF NAO index categorization. Considerable spatial similarity between the DJF and MAM maps is found for MSLP, SAT, and precipitation fields. Furthermore, the observed spring (MAM) SST anomaly pattern in the North Atlantic is significantly correlated with the NAO index of the preceding winter (DJF) season.

A physical mechanism enabling such a time-delayed NAO impact is explored by employing the ICTP AGCM coupled with a slab-ocean layer in the North Atlantic (NATL run). When compared with the observed atmospheric response, it is shown that the NATL run adequately simulates both DJF and MAM responses and reproduces the SST pattern consistently with the observations. A SST dipole pattern in the extratropical Atlantic is proposed as a possible link between the DJF NAO and the subsequent spring climate over Europe. The connection between the North Atlantic SST dipole and the DJF NAO is examined using SSTI, an index defined in such a way that it measures the strength of the dipole. The correlations between the DJF NAO and the monthly SSTIs reveal a clear asymmetry in the lead–lag correlation, with larger values if the DJF NAO is leading the SSTI, suggesting a DJF NAO forcing of the spring

SSTI. According to the presented results, the wintertime midlatitude SST dipole persists for several months, allowing thermal coupling between the ocean and atmosphere. As a result, a springtime atmospheric response similar to the wintertime NAO pattern is found in both the observations and the NATL experiment. Such an SST pattern is not reproduced in the CLIM run by construction (the ICTP AGCM run with no ocean–atmosphere coupling). The observed MAM SLP pattern projects onto the DJF SLP pattern with high spatial correlation and the same is also found for SLP simulated by the NATL run. Contrarily, for the experiment performed with the AGCM with no slab ocean (CLIM), the MAM SLP pattern projects onto the DJF pattern only over the ocean while is significantly different over Europe. This result indicates the mixed layer SSTs are a contributing link in the temporal teleconnectivity of the wintertime NAO and the spring climate over Europe.

Note that some other mechanisms apart from the midlatitude SST forcing in the North Atlantic and its associated interactions with the atmosphere may also contribute to prolonged NAO-related climate anomalies over Europe (e.g., processes that include sea ice, snow, soil moisture, tropical/subtropical influences, etc.). In other words, the midlatitude SST pattern in the North Atlantic examined in this study is not the only factor participating in the temporal teleconnection between

the wintertime NAO and spring climate. For example, the atmosphere in the North Atlantic sector is sensitive to sea ice variations with the large-scale atmospheric response resembling an NAO pattern (Deser et al. 2000, 2007). However, in our study sea ice is prescribed as climatological (only seasonally varying) values and therefore the influence of the interannual variations in sea ice is not included in the analysis of the modeled atmospheric response. Indeed, observed circulation anomalies reflect not only the extratropical SST impact that is in the focus of the study, but also other processes occurring in nature (e.g., sea ice variations, tropical influence, etc.). Nevertheless, the presented results indicate extratropical SSTs as a contributing factor in the connection between the wintertime NAO and the following springtime climate. It is demonstrated here that the atmospheric circulation associated with the DJF NAO generates an SST anomaly pattern in the North Atlantic, which can subtly affect the atmospheric circulation over Europe during the following spring.

However, when the obtained results are interpreted, their probable discrepancies from reality in amplitude, as well as in the precise positioning of the atmospheric response, due to model's simplicity and coarse resolution, should be taken into consideration. Still, it is encouraging that even an intermediate-complexity model is capable of reproducing an extratropical SST effect on the atmospheric circulation similar to the observations. We believe that state-of-the-art models should give even better results, but using the relatively simple ICTP AGCM is justified on the grounds that it has the ability to reproduce the atmospheric mean state and NAO-related circulation reasonably well. It is also important from a practical point of view that a simple model makes it possible to perform many sensitivity experiments in order to separate different factors that contribute to air-sea interaction.

*Acknowledgments.* The manuscript greatly benefited from the comments and suggestions of Prof. Daniel J. Vimont and anonymous reviewers. This work was supported in part by the University Development Fund, University of Zagreb (Grant 198005), and the Ministry of Science, Educational and Sports of the Republic of Croatia (Grant 119-1193086-1323).

#### REFERENCES

- Allan, R., and T. Ansell, 2006: A new globally complete monthly historical gridded mean sea level pressure dataset (HadSLP2): 1850–2004. *J. Climate*, **19**, 5816–5842.
- Barnston, A. G., and R. E. Livezey, 1987: Classification, seasonality and persistence of low-frequency atmospheric circulation patterns. *Mon. Wea. Rev.*, **115**, 1083–1126.
- Barsugli, J. J., and D. S. Battisti, 1998: The basic effects of atmosphere–ocean thermal coupling on midlatitude variability. *J. Atmos. Sci.*, **55**, 477–493.
- Basnett, T., and D. Parker, 1997: Development of the Global Mean Sea Level Pressure Data Set GMSLP2. Climate Research Tech. Note 79, 16 pp. [Available from Hadley Centre, Met Office, FitzRoy Road, Exeter, Devon EX1 3PB, United Kingdom.]
- Bjerknes, J., 1964: Atlantic air–sea interaction. *Advances in Geophysics*, Vol. 10, Academic Press, 1–82.
- Bladé, I., 1997: The influence of midlatitude ocean–atmosphere coupling on the low-frequency variability of a GCM. Part I: No tropical SST forcing. *J. Climate*, **10**, 2087–2106.
- Bracco, A., F. Kucharski, R. Kallummal, and F. Molteni, 2004: Internal variability, external forcing and climate trends in multidecadal AGCM ensembles. *Climate Dyn.*, **23**, 659–678.
- Bretherton, C. S., and D. S. Battisti, 2000: An interpretation of the results from atmospheric general circulation models forced by the time history of the observed sea surface temperature distribution. *Geophys. Res. Lett.*, **27**, 767–770.
- Brohan, P., J. J. Kennedy, I. Harris, S. F. B. Tett, and P. D. Jones, 2006: Uncertainty estimates in regional and global observed temperature changes: A new dataset from 1850. *J. Geophys. Res.*, **111**, D12106, doi:10.1029/2005JD006548.
- Cassou, C., C. Deser, and M. A. Alexander, 2007: Investigating the impact of reemerging sea surface temperature anomalies on the winter atmospheric circulation over the North Atlantic. *J. Climate*, **20**, 3510–3526.
- Cayan, D. R., 1992a: Latent and sensible heat flux anomalies over the northern oceans: Driving the sea surface temperature. *J. Phys. Oceanogr.*, **22**, 859–881.
- , 1992b: Latent and sensible heat flux anomalies over the northern oceans: The connection to monthly atmospheric circulation. *J. Climate*, **5**, 354–369.
- Czaja, A., and C. Frankignoul, 1999: Influence of the North Atlantic SST on the atmospheric circulation. *Geophys. Res. Lett.*, **26**, 2969–2972.
- , and J. Marshall, 2000: On the interpretation of AGCMs response to prescribed time-varying SST anomalies. *Geophys. Res. Lett.*, **27**, 1927–1930.
- de Boyer-Montégut, C., G. Madec, A. S. Fischer, A. Lazar, and D. Iudicone, 2004: Mixed layer depth over the global ocean: An examination of profile data and a profile-based climatology. *J. Geophys. Res.*, **109**, C12003, doi:10.1029/2004JC002378.
- Deser, C., and M. L. Blackmon, 1993: Surface climate variations over the North Atlantic Ocean during winter: 1900–89. *J. Climate*, **6**, 1743–1753.
- , and M. S. Timlin, 1997: Atmosphere–ocean interaction on weekly timescales in the North Atlantic and Pacific. *J. Climate*, **10**, 393–408.
- , J. E. Walsh, and M. S. Timlin, 2000: Arctic sea ice variability in the context of recent atmospheric circulation trends. *J. Climate*, **13**, 617–633.
- , R. A. Tomas, and S. Peng, 2007: The transient atmospheric circulation response to North Atlantic SST and sea ice anomalies. *J. Climate*, **20**, 4751–4767.
- Eden, C., and T. Jung, 2001: North Atlantic interdecadal variability: Oceanic response to the North Atlantic Oscillation (1865–1997). *J. Climate*, **14**, 676–691.
- , and J. Willebrand, 2001: Mechanism of interannual to decadal variability of the North Atlantic circulation. *J. Climate*, **14**, 2266–2280.

- Ferreira, D., and C. Frankignoul, 2005: The transient atmospheric response to midlatitude SST anomalies. *J. Climate*, **18**, 1049–1067.
- Fischer, E. M., S. I. Seneviratne, D. Lüthi, and C. Schär, 2007: Contribution of land–atmosphere coupling to recent European summer heat waves. *Geophys. Res. Lett.*, **34**, L06707, doi:10.1029/2006GL029068.
- Folland, C. K., J. Knight, H. W. Linderholm, D. Fereday, S. Ineson, and J. W. Hurrell, 2009: The summer North Atlantic oscillation: Past, present, and future. *J. Climate*, **22**, 1082–1103.
- Frankignoul, C., 1985: Sea surface temperature anomalies, planetary waves and air–sea feedback in the middle latitudes. *Rev. Geophys.*, **23**, 357–390.
- , and K. Hasselmann, 1977: Stochastic climate models, II, Application to sea surface temperature variability and thermocline variability. *Tellus*, **29**, 284–305.
- , A. Czaja, and B. L'Hévéder, 1998: Air–sea feedback in the North Atlantic and surface boundary conditions for ocean models. *J. Climate*, **11**, 2310–2324.
- , N. Sennéchaël, Y.-O. Kwon, and M. A. Alexander, 2011: Influence of the meridional shifts of the Kuroshio and the Oyashio extensions on the atmospheric circulation. *J. Climate*, **24**, 762–777.
- Greatbatch, R. J., and T. Jung, 2007: Local versus tropical heating and winter North Atlantic Oscillation. *J. Climate*, **20**, 2058–2075.
- Herceg-Bulić, I., and F. Kucharski, 2011: Delayed ENSO impact on spring precipitation over North/Atlantic European region. *Climate Dyn.*, **38**, 2593–2612.
- Hurrell, J. W., 1996: Influence of variations in extratropical wintertime teleconnections on Northern Hemisphere temperature. *Geophys. Res. Lett.*, **23**, 665–668.
- , Y. Kushnir, and G. Ottersen, 2003: An overview of the North Atlantic oscillation. *The North Atlantic Oscillation: Climatic Significance and Environmental Impact*, *Geophys. Monogr.*, Vol. 134, Amer. Geophys. Union, 1–35, doi:10.1029/134GM01.
- Jung, T., F. Vitart, L. Ferranti, and J.-J. Morcrette, 2011: Origin and predictability of the extreme negative NAO winter of 2009/10. *Geophys. Res. Lett.*, **38**, L07701, doi:10.1029/2011GL046786.
- Kucharski, F., and F. Molteni, 2003: On non-linearities in a forced North Atlantic Oscillation. *Climate Dyn.*, **21**, 677–687.
- , —, and J. H. Yoo, 2006: SST forcing of decadal Indian monsoon rainfall variability. *Geophys. Res. Lett.*, **33**, L03709, doi:10.1002/2005GL025371.
- , —, M. P. King, R. Farneti, I.-S. Kang, and L. Feudale, 2013: On the need of intermediate complexity general circulation models: A “SPEEDY” example. *Bull. Amer. Meteor. Soc.*, **94**, 25–30.
- Kushnir, Y., 1994: Interdecadal variations in North Atlantic sea surface temperature and associated atmospheric conditions. *J. Climate*, **7**, 141–157.
- , and I. M. Held, 1996: On the equilibrium atmospheric response to North Atlantic SST anomalies. *J. Climate*, **9**, 1208–1220.
- , W. A. Robinson, I. Bladé, N. M. J. Hall, S. Peng, and R. Sutton, 2002: Atmospheric GCM response to extratropical SST anomalies: Synthesis and evaluation. *J. Climate*, **15**, 2233–2256.
- Mitchell, T. D., T. R. Carter, P. D. Jones, M. Hulme, and M. New, 2004: A comprehensive set of high-resolution grids of monthly climate for Europe and the globe: The observed record (1901–2000) and 16 scenarios (2001–2100). Tyndall Centre for Climate Change Research Working Paper 55, 25 pp. [Available online at <http://www.tyndall.ac.uk/sites/default/files/wp55.pdf>.]
- Molteni, F., 2003: Atmospheric simulations using a GCM with simplified physical parameterizations. I: Model climatology and variability in multi-decadal experiments. *Climate Dyn.*, **20**, 175–191.
- Mosedale, T. J., D. B. Stephenson, M. Collins, and T. C. Mills, 2006: Granger causality of coupled climate processes: Ocean feedback on the North Atlantic Oscillation. *J. Climate*, **19**, 1182–1194.
- New, M., M. Hulme, and P. D. Jones, 2000: Representing twentieth-century space–time climate variability. Part II: Development of 1901–96 monthly grids of terrestrial surface climate. *J. Climate*, **13**, 2217–2238.
- Ogi, M., Y. Tachibana, and K. Yamazaki, 2003: Impact of the wintertime North Atlantic Oscillation (NAO) on the summertime atmospheric circulation. *Geophys. Res. Lett.*, **30**, 1704, doi:10.1029/2003GL017280.
- Peng, S., and J. S. Whitaker, 1999: Mechanisms determining the atmospheric response to midlatitude SST anomalies. *J. Climate*, **12**, 1393–1408.
- Rigor, I. G., J. M. Wallace, and R. L. Colony, 2002: On the response of sea ice to the Arctic Oscillation. *J. Climate*, **15**, 2648–2663.
- Rodwell, M. J., and C. K. Folland, 2002: Atlantic air–sea interaction and seasonal predictability. *Quart. J. Roy. Meteor. Soc.*, **128**, 1413–1443.
- , D. P. Rowell, and C. K. Folland, 1999: Oceanic forcing of the wintertime North Atlantic Oscillation and European climate. *Nature*, **398**, 320–333.
- Rogers, J. C., 1990: Patterns of low-frequency monthly sea level pressure variability (1899–1986) and associated wave cyclone frequencies. *J. Climate*, **3**, 1364–1379.
- , 1997: North Atlantic storm track variability and its association to the North Atlantic Oscillation and climate variability of northern Europe. *J. Climate*, **10**, 1635–1647.
- Scaife, A. A., J. R. Knight, G. K. Vallis, and C. K. Folland, 2005: A stratospheric influence on the winter NAO and North Atlantic surface climate. *Geophys. Res. Lett.*, **32**, L18715, doi:10.1029/2005GL023226.
- , and Coauthors, 2011: Improved Atlantic winter blocking in a climate model. *Geophys. Res. Lett.*, **38**, L23703, doi:10.1029/2011GL049573.
- Seager, R., Y. Kushnir, M. Visbeck, N. Naik, J. Miller, G. Krahnmann, and H. Cullen, 2000: Causes of Atlantic Ocean climate variability between 1958 and 1998. *J. Climate*, **13**, 2845–2862.
- Serreze, M. C., F. Carse, R. G. Barry, and J. C. Rogers, 1997: Icelandic low cyclone activity: Climatological features, linkages with the NAO, and relationships with recent changes in the Northern Hemisphere circulation. *J. Climate*, **10**, 453–464.
- Smith, T. M., R. W. Reynolds, T. C. Peterson, and J. Lawrimore, 2008: Improvements to NOAA’s historical merged land-ocean surface temperature analysis (1880–2006). *J. Climate*, **21**, 2283–2296.
- Sutton, R. T., W. A. Norton, and S. P. Jewson, 2001: The North Atlantic Oscillation—What role for the ocean? *Atmos. Sci. Lett.*, **1**, 89–100.
- Vautard, R., and Coauthors, 2007: Summertime European heat and drought waves induced by wintertime Mediterranean rainfall deficit. *Geophys. Res. Lett.*, **34**, L07711, doi:10.1029/2006GL028001.

- Visbeck, M., E. Chassignet, R. Curry, T. Delworth, B. Dickson, and G. Krahnemann, 2003: The ocean's response to North Atlantic oscillation variability. *The North Atlantic Oscillation, Geophys. Monogr.*, Vol. 134, Amer. Geophys. Union, 113–146.
- Walker, G. T., 1924: Correlation in seasonal variations of weather, IX. A further study of world weather. *Mem. Ind. Meteor. Dept.*, **24**, 275–333.
- , and E. W. Bliss, 1932: World weather V. *Mem. Roy. Meteor. Soc.*, **4** (36), 53–84.
- Wang, W., B. T. Anderson, R. K. Kaufmann, and R. B. Myeni, 2004: The relation between the North Atlantic Oscillation and SSTs in the North Atlantic basin. *J. Climate*, **17**, 4752–4759.
- Watanabe, M., and M. Kimoto, 2000: Atmosphere–ocean thermal coupling in the North Atlantic: A positive feedback. *Quart. J. Roy. Meteor. Soc.*, **126**, 3343–3369.
- Woollings, T., B. J. Hoskins, M. Blackburn, and P. Berrisford, 2008: A new Rossby wave–breaking interpretation of the North Atlantic Oscillation. *J. Atmos. Sci.*, **65**, 609–626.

Copyright of Journal of Climate is the property of American Meteorological Society and its content may not be copied or emailed to multiple sites or posted to a listserv without the copyright holder's express written permission. However, users may print, download, or email articles for individual use.